Colored Activity in Self-Organized Critical Interface Dynamics

Kim Sneppen and Mogens H. Jensen
Niels Bohr Institute and NORDITA, Blegdamsvej 17, DK-2100 Copenhagen Ø, Denmark
(Received 26 February 1993)

We study roughening interfaces that become self-organized critical by a rule similar to that of invasion percolation. We demonstrate that there is a fundamental difference between transient and critical dynamical exponents. The exponents break the Galilean invariance and temporal multiscaling is observed. We show that the activity along the interface exhibits nontrivial power law correlations in both space and time even though only quenched Gaussian noise is applied. The results are compared with simulations where spatial power law correlated noise is used as input.

PACS numbers: 68.35.Fx, 05.70.Ln, 47.55.Mh, 68.45.Gd

Dynamically roughening interfaces have been studied quite intensively in recent years using stochastic [such as Kardar-Parisi-Zhang (KPZ)] [1] and deterministic (such as Kuramoto-Sivashinsky) [2] differential equations as well as by various deposition models [3,4]. In addition, many experiments on roughening interfaces have been performed on porous media, burning paper, fluid penetration in paper, etc.; see Refs. [5–12]. It was observed that the roughening exponents found in the experiments often were quite distinct from the theoretically predicted exponents. Some authors [13,14] explained this discrepancy by models where a power law behavior in the additive or quenched noise of the system was introduced from *outside*. Subsequently, a power law distribution of the effective additive noise was measured experimentally in Ref. [15].

Recently, however, Sneppen [16] introduced a simple growth model where the motion of the interface is determined by a rule similar to that of invasion percolation [17]. Reference [18] also mentions an interface model of this type. The static roughening exponent was found to be $\chi = 0.63 \pm 0.02$, in reasonable agreement with experimental results. In this Letter we study the values of the saturated exponents and the spatial-temporal correlations of the activity generated by the dynamics at saturation. We observe power law scaling of this activity and believe it represents the first example of an interface model which generates nontrivial power law activity (effective noise) without any power law as "input."

The model is defined on a lattice where each lattice point (x, h) is assigned a quenched uncorrelated Gaussian random number $\eta(x, h)$. In the one-dimensional version a discrete interface $h(x)$ is defined on a discrete chain $x = 1, 2, 3 \ldots L$. We use periodic boundary conditions. The chain is updated by finding the site with the smallest random number $\eta(x, h(x))$ among all sites on the interface. On this site one unit is added to h. Then neighboring sites are adjusted upwards ($h \to h + 1$) precisely until all slopes $|h(x) - h(x-1)| \leq 1$. The dynamics mimics the motion of, say, the interface of oil penetrating a porous medium. Here progress is often observed to occur in local avalanches.

A main result of Ref. [16] was a numerical calculation of the scaling of the interface width with time t and system size L. Thus, as also shown in Fig. 1(a), the width $w = \langle (h - \langle h \rangle)^2 \rangle^{1/2}$ of a saturated interface scales with

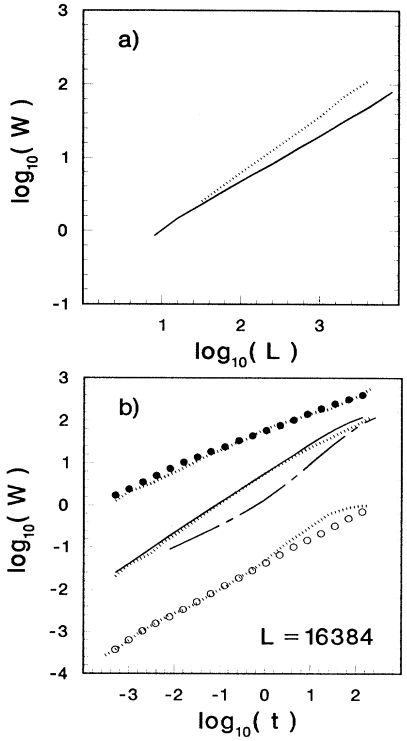

FIG. 1. (a) Width vs system size L. The full line shows results from the model, and the dotted line the behavior of the LFI with f=1.25. As described in the text, the LFI is a random activation interface model with power law jumps. (b) Scaling of height-height correlations with time (for system size $L = 16\,384$): The dashed-full line shows the transient development of the interface. The full line shows the behavior at saturation. The big black circles reveal the ∞ moment $H(t)$ of the height-height correlations whereas the open circles show the zeroth moment, counting the fraction of activated sites. The dotted lines display the corresponding scalings for the LFI at saturation.

0031-9007/93/71(1)/101(4)$06.00

system size L^{χ} with $\chi = 0.63 \pm 0.02$. As noted in [16] this scaling may be understood from a self-organization of the interface towards a "critical" attractor which consists of an ensemble of directed percolating strings (of high values of η) at their critical point. In Ref. [19] it is demonstrated that the distribution of η along a saturated interface indeed agrees with this. For interface dynamics near a critical point, see also [12,20]. It is interesting to note that the temporal drift of the interface towards a critical state in this model can be viewed as a simple example of self-organized criticality [21] which here takes place also in 1D [22].

In Ref. [16] it was furthermore demonstrated that the transient roughening is fast, exhibiting nearly linear growth with time; see Fig. 1(b). As the transient is the motion towards, but not at, the critical attractor, one may, however, expect that the dynamical exponent in the saturated state is different. Measuring the height-height time correlations by

$$W(L,t) = \langle [h(x,t+\tau) - h(x,\tau)] - \langle h(x,t+\tau) - h(x,\tau)\rangle^2 \rangle^{1/2} \quad (1)$$

(average $\langle\ \rangle$ over $x \in [1,L]$ and members of the ensemble), we plot in Fig. 1(b) the temporal behavior starting from both a flat interface and a critical (saturated) state. We observe a dramatic difference, with a critical state time correlation [23]:

$$W(L,t) \propto t^{\beta_{\rm crit}} \quad \text{with} \quad \beta_{\rm crit} = 0.69 \pm 0.02\ . \quad (2)$$

This is to our knowledge the first time that an interface model shows widely different predictions of transient and saturated time scalings. Also we find that the interface motion clearly breaks the Galilean invariance [1] because $\chi + \chi/\beta_{\rm crit} = 1.56 \pm 0.05$. The open circles show that the fraction of activated sites (equals the zeroth moment of the activity) scales as $N(t) \propto t^{0.58\pm0.02}$. The solid circles display the temporal behavior of the infinite moment of the height-height correlation function

$$H(t) = \langle |\max_x \{h(x,t+\tau) - h(x,\tau)\} - \min_x \{h(x,t+\tau) - h(x,\tau)\}| \rangle_\tau\ , \quad (3)$$

with $x \in [1,L]$ and the average $\langle\ \rangle$ taken over ensemble members at various times τ after saturation. We observe that

$$H(t) \propto t^{\beta^{\infty}_{\rm crit}} \quad \text{with} \quad \beta^{\infty}_{\rm crit} = 0.41 \pm 0.02\ , \quad (4)$$

which is significantly different from the scaling of the second moment W [24], in contrast to the temporal behavior of the model of Ref. [20]. We call this behavior temporal multiscaling, in contrast to spatial multiscaling [25] which is not observed in this model [16].

A main ingredient in the model is that one keeps a one-dimensional directed interface without overhangs, thus making the distribution of activities along this interface especially simple to study. We describe the activity in terms of events on a critical string: An event starts by finding the site with minimal η along the interface. This initiates a local avalanche which, as demonstrated in Fig. 2, has a characteristic size (defined as the number of adjusted sites). Let $x(t)$ and $x(t+dt)$ be the positions of the event at time t and $t+dt$, respectively. With $dt = 1/L$ we consider the proceeding event after the event occurring at t; if $dt = 2/L$ the second event after t is considered, etc., and calculate the probability distribution function $P(X_{dt})$ in the variable $X_{dt} = |x(t) - x(t+dt)|$. In Fig. 3(a) this distribution function is shown for different values of dt, $dt = \frac{1}{L}$, $\frac{2}{L}$, $\frac{4}{L}$, $\frac{10}{L}$, and $\frac{100}{L}$. We obtain a very good power law scaling

$$P_X(X_{dt}) = A(X_{dt},dt)\, X_{dt}^{-\gamma}\ , \quad (5)$$

where $\gamma = 2.25 \pm 0.05$, independent of the value of dt.

In Fig. 3(b) we have for a given point measured the probability distribution function of time differences t between successive local events at this point. One observes that this distribution also exhibits a reasonable scaling

$$P_{\rm First}(t) \propto t^{-\tau_F}\ , \quad (6)$$

with the nontrivial exponent $\tau_F \approx 1.2 \pm 0.1$ (for times $1/L << t << 1$). We remember that if the activity along the interface exhibited a random walk with bounded step sizes, then $P_{\rm First}(t) \propto t^{-1.5}$ corresponds to the distribution of first return times for random walkers. Thus, as $\tau < \frac{3}{2}$, the motion of activity is less constrained than a finite step random walker. Also note that in Fig. 3(b) we display, at saturation, the chance of activity in a point X, at a time $t+\tau$, given there has been activity in X at

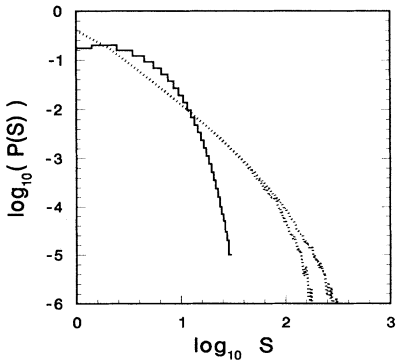

FIG. 2. Size distribution of local avalanches in the model and in a LFI with $f = 1.25$. The various dotted lines indicate different system sizes in the LFI; $L = 1024$ and 4096, respectively.

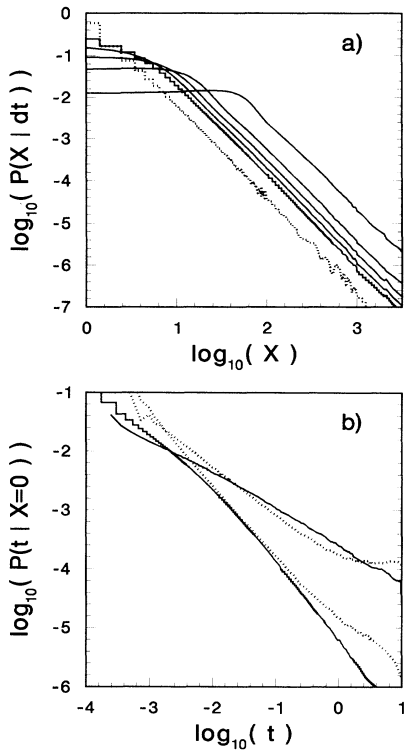

FIG. 3. (a) Spatial distribution Eq. (3) of activity centers, separated in time by $dt = 1/L$, $2/L$, $4/L$, $10/L$, and $100/L$ where the system size $L = 8192$. The dotted line shows the *input* activity in a LFI with $f = 1.25$ with slope $-\gamma = -f - 1 = -2.25$ (as sampled during the numerical computation), made to fit the scaling of the model. (b) Probability for activity in a given site as a function of time: "Steep" full line: first return; "flat" full line: all returns. The dotted lines are the corresponding LFI results.

time τ. We observe

$$P_{\text{Activ}}(t) \propto t^{-\tau_A} , \tag{7}$$

with exponent $\tau_A = 0.62 \pm 0.04$ resembling the scaling of activated sites $N(t) \propto t^{0.58\pm0.02}$, suggesting that temporal spreading of activity balances the decrease in the local probability of activity. We stress that the power laws in Eqs. (4), (5), and (6) are in sharp contrast to the normally studied cases [1,3], with uncorrelated noise implying that these distributions are flat.

It is tempting to relate the measured temporal and spatial activity correlations by simply assuming that the motion of activity performs a Levy flight of uncorrelated subsequent jumps [4], with a jump length given by a Levy flight exponent f:

$$P_{\text{Levy}}(X)\, dX = X^{-f-1}\, dX . \tag{8}$$

From comparison with the measured spatial activity correlation in the model, we are particularly interested in $f = \gamma - 1 = 1.25 \pm 0.05$. In a Levy flight subsequent jumps are separated by a distance $X \in [1, L/2]$ given by $X \propto \eta^{-1/f}$, where η is a random number uniformly distributed between 0 and 1. The direction of the jump is chosen randomly. Using a Levy flight with $f = 1.25$ to locate the next activity center, we thereafter add one unit at this center ($h \to h+1$) followed by adjustment of neighbor sites precisely until all slopes remain less than or equal to 1 (periodic boundary conditions). We call this model the Levy flight interface model (LFI). In Figs. 1(a) and 1(b) the dotted curves show the results of the LFI. As seen in these figures, the temporal roughening of the model is approximately reproduced by the LFI whereas the measured $\chi_{\text{LFI}} = 0.78 \pm 0.05$ is significantly different from that of the model. In Fig. 2 we furthermore see that, in contrast to the model, avalanches in the LFI are nonlocal, in the sense that their size is power law distributed with a cutoff dependent on the system size. In Fig. 3(b) we have indicated with dots that the scaling of the first return times of the activity in the LFI roughly matches the behavior of the model, whereas the scaling of all returns fails completely (see [26]).

In order to understand the difference in the large scale behavior between the LFI and the model, we have studied correlations between subsequent jumps. It appears that these are highly correlated in the model, whereas a basic assumption of the LFI is uncorrelated subsequent jumps. To be specific, we define for two intervals Δ_1, Δ_2:

$$C(\Delta_1, \Delta_2) = \frac{p(\mathbf{v}_1 \cdot \mathbf{v}_2 > 0) - p(\mathbf{v}_1 \cdot \mathbf{v}_2 < 0)}{p(\mathbf{v}_1 \cdot \mathbf{v}_2 > 0) + p(\mathbf{v}_1 \cdot \mathbf{v}_2 < 0)} , \tag{9}$$

$$|\mathbf{v}_1| \in \Delta_1 , \quad |\mathbf{v}_2| \in \Delta_2 ,$$

where $\mathbf{v}_1$ and $\mathbf{v}_2$ are subsequent jump vectors of activity centers and p denotes the corresponding probability. For $\Delta_1, \Delta_2 = [0, L/4]$ with system size L large, we obtain numerically $C(\Delta_1, \Delta_2) = -0.055 \pm 0.005$ whereas, for LFI, $C \equiv 0$ always. If one considers large jumps only, we obtain $C \approx -0.8$, thus reflecting the enhanced probability of making subsequent reverse jumps between activity centers that are widely separated. Furthermore, C turns out not to be symmetric in (Δ_1, Δ_2). Investigations of the three jump correlations also reveal significant additional correlations. This altogether indicates that the large scale dynamics of the model is not given entirely by only one exponent f. Indeed both the static exponent χ and the temporal activity exponent τ_A are not compatible with the LFI.

Finally we would like to stress the fact that the model breaks the Galilean invariance. In usual descriptions of large scale evolution of interfaces in terms of the KPZ equation [1],

$$\frac{dh}{dt} = \Delta h + \lambda \left(\frac{dh}{dx}\right)^2 + \eta(x,t) , \tag{10}$$

the Galilean invariance ($\chi + \chi/\beta = 2$) is imposed by

the nonlinear term. We do not know whether the dynamics of the present model can be described by such a Langevin equation, but within such a framework Medina *et al.* [27] demonstrated that for a stochastic noise η with sufficiently strong power law temporal correlations the Galilean invariance would be broken; in fact they show that $\chi + \chi/\beta > 2$. Our model, as well as the LFI, breaks the Galilean invariance by $\chi + \chi/\beta_{\text{crit}} < 2$, thus reflecting a fundamental difference between the additive noise considered by Medina *et al.* [27] and our subsequent activity of separated events. This difference might also be reflected by the presence of temporal multiscaling in our model that is connected with the accumulation of subsequent local activity in separated regions of the string [28].

We conclude by emphasizing the interesting dynamical and spatial power law correlations that naturally appear in the critical state of an interface that develops according to the present model. Whereas the roughness exponent χ reflects the scaling of the transverse with the longitudinal correlation length in directed percolation [16], the other exponents, such as γ, β_{crit}, $\beta^{\infty}_{\text{crit}}$, and τ_A, are at present without any such analogies to directed percolation. Comparison to a Levy flight interface model has demonstrated that using only the spatial correlation exponent γ as input, we approximately reproduce the exponents β_{crit} and $\beta^{\infty}_{\text{crit}}$ but not χ and τ_A.

Horvath, Family, and Vicsek [15] have, for flows through porous media, experimentally extracted a power law distribution of global additive noise. However, we think that measurements of the distribution of spatial distances between possible subsequent local avalanches could establish a new way of analyzing some roughening interface phenomena.

K. Sneppen is grateful to the Carlsberg Foundation for financial support and we have both benefited from discussions with T. Bohr, H. Fogedby, H.J. Jensen, and Y.-C. Zhang.

[1] M. Kardar, G. Parisi, and Y.-C. Zhang, Phys. Rev. Lett. **56**, 889 (1986).

[2] I. Procaccia, M.H. Jensen, V.S. L'vov, K. Sneppen, and R. Zeitak, Phys. Rev. A **46**, 3220 (1992); K. Sneppen, J. Krug, M.H. Jensen, C. Jayaprakash, and T. Bohr, Phys. Rev. A **46**, R7351 (1992).

[3] J.M. Kim and J.M. Kosterlitz, Phys. Rev. Lett. **62**, 2289 (1989).

[4] P. Meakin and R. Jullien, Phys. Rev. A **41**, 983 (1990); A. Magnolia and H.E. Warriner, J. Stat. Phys. **60**, 809 (1990).

[5] G.B. Springfellow, Rep. Prog. Phys. **45**, 469 (1982); G. Davies, Phys. Bull. **39**, 22 (1988); G.S. Bales, A.C. Redfield, and A. Zangwill, Phys. Rev. Lett. **62**, 776 (1989).

[6] L.M. Galathara, K.S. Kahanda, Xiao-qun Zou, R. Farral, and Po-zen Wong, Phys. Rev. Lett. **68**, 3741 (1992).

[7] M. Siegert and M. Plischke, Phys. Rev. Lett. **68**, 2035 (1992); for an overview, see *Kinetics of Ordering and Growth at Surfaces*, edited by M. Legally (Plenum, New York, 1990).

[8] T. Vicsek, M. Cserzö, and V.K. Horváth, Physica (Amsterdam) **167A**, 315 (1990).

[9] M.A. Rubio, C. Edwards, A. Dougherty and J.P. Gollup, Phys. Rev. Lett. **63**, 1685 (1989); **65**, 1389 (1990).

[10] V.K. Horváth, F. Family, and T. Vicsek, Phys. Rev. Lett. **65**, 1388 (1990), J. Phys. A **24**, L25 (1991).

[11] J. Zhang, Y.-C. Zhang, P. Alstroem, and M.T. Levinsen, Physica (Amsterdam) **189A**, 383 (1992).

[12] S. V. Buldyrev, A.-L. Barabási, F. Caserta, S. Havlin, H. E. Stanley, and T. Vicsek, Phys. Rev. A **45**, R8313 (1992).

[13] Y.-C. Zhang, J. Phys. (Paris) **51**, 2129 (1990).

[14] M.H. Jensen and I. Procaccia, J. Phys. II (France) **1**, 1139 (1991).

[15] V.K. Horvath, F. Family, and T. Vicsek, Phys. Rev. Lett. **67**, 3207 (1991).

[16] K. Sneppen, Phys. Rev. Lett. **69**, 3539 (1992).

[17] D. Wilkinson and J.F. Willemsen, J. Phys. A **16**, 3365 (1983).

[18] S. Havlin, A.-L. Barabási, S.V.C. Buldyrev, K. Peng, M. Schwartz, H.E. Stanley, and T. Vicsek, in *Proceedings of the Granada Conference on Fractals*, edited by P. Meakin and L. Sander (Plenum, New York, 1992).

[19] Lei-Han Tang and H. Leschhorn (to be published).

[20] L.-H. Tang and H. Leschhorn, Phys. Rev. A **45**, R8309 (1992).

[21] P. Bak, C. Tang, and K. Wiesenfeld, Phys. Rev. Lett. **59**, 381 (1987); C. Tang and P. Bak, Phys. Rev. Lett. **60**, 2347 (1988).

[22] S. Nagel, L.P. Kadanoff, L. Wu, and S. Zhou, Phys. Rev. A **39**, 6524 (1989).

[23] Comparing to two other interface models (which both allow for infinite slopes) on lattices tuned from outside at the critical point for directed percolation, we find the same β value as Ref. [12] but different from Ref. [20].

[24] A.-L. Barabási, J. Phys. A **24**, L1013 (1991); Y.-C. Zhang, J. Phys. I (France) **2**, 2175 (1992).

[25] A.-L. Barabási and T. Vicsek, Phys. Rev. A **44**, 2730 (1991); A.-L. Barabási, P. Szépfalusy, and T. Vicsek, Physica (Amsterdam) **178A**, 17 (1991).

[26] A Levy flight with spatial exponent $f = 1.25$ will have a first passage probability with temporal exponent $\tau^p_F(\text{Levy}) = 2 - 1/f = 1.2$ and passage probability at all with temporal exponent $\tau^p_A(\text{Levy}) = 1/f = 0.8$ [see H.C. Fogedby, T. Bohr, and H.J. Jensen, J. Stat. Phys. **66**, 583 (1992)]. These Levy flight exponents agree with ones deduced from dotted lines in Fig. 3(b); i.e., upon passage there is a fixed constant probability for hitting. Comparison of LFI with temporal scalings in the studied model reveals reasonable agreement for first return, but fails completely the scaling of activity at all returns.

[27] E. Medina, T. Hwa, M. Kardar, and Y-C. Zhang, Phys. Rev. A **39**, 3053 (1989).

[28] M.H. Jensen and K. Sneppen, in Proceedings of the Santa Fe NATO Advanced Research Workshop on Spatio-Temporal Pattern Formation and Complexity (to be published).